

## **A STRUCTURAL RELIABILITY FRAMEWORK FOR COLLAPSE RISK ASSESSMENT INCORPORATING GROUND MOTION DURATION AND RESPONSE SPECTRAL SHAPE**

Reagan Chandramohan\*

### **ABSTRACT**

A structural reliability framework is developed to post-process the results of an incremental dynamic analysis (IDA) and compute a hazard-consistent collapse fragility curve. The ability to produce hazard-consistent collapse risk estimates eliminates a major drawback in the IDA procedure and brings its capabilities on par with multiple stripe analysis (MSA). The proposed framework uses two secondary ground motion intensity measures:  $S_aRatio$ , which is used to quantify response spectral shape and 5-75% significant duration ( $DS_{5-75}$ ). Both  $S_aRatio$  and  $DS_{5-75}$  are demonstrated to be efficient predictors of a ground motion's collapse intensity, which is a measure of its potential to cause structural collapse. In the case of the ductile eight-story reinforced concrete moment frame building analyzed in this study, they are capable of explaining 81% of the variance in the ground motion collapse intensities. The collapse fragility curve estimated using this framework is found to compare well to the fragility curve obtained by conducting MSA using hazard-consistent ground motions. MSA is shown to represent a simulation-based approach to solve the same structural reliability problem. Finally, optimal ground motion selection strategies to produce accurate collapse risk estimates are proposed.

### **INTRODUCTION**

Incremental dynamic analysis (IDA) (Vamvatsikos and Cornell 2002) is a popular analysis procedure for estimating structural collapse risk under earthquake ground motions. It involves scaling each ground motion from a set to incrementally higher intensity levels, until structural collapse is observed. A number of recent studies have highlighted the importance of using ground motions for structural performance assessment, that are representative of the seismic hazard at the site under consideration (Bommer and Acevedo 2004, Katsanos et al. 2010). This implies using ground motions whose characteristics, like frequency content, duration, and the presence or absence of velocity pulses, match the range of characteristics of the ground motions anticipated at the site. Since ground motions of different intensities are expected to have different characteristics, ideally, this requires analyzing the structure under different sets of hazard-consistent ground motions at different intensity levels. Hence, structural risk estimates obtained using IDA, where the same set of ground motions is scaled to different intensity levels, are often inaccurate. FEMA P695 (FEMA 2009) attempts to address this problem by using an approximate, empirically calibrated spectral shape factor to adjust the median collapse capacity estimated by conducting IDA with a prescribed far-field record set. Multiple stripe analysis

---

\* Doctoral Candidate, Dept. of Civil and Environmental Engineering, Stanford University, Stanford, CA 94305

(MSA) (Jalayer 2003), on the other hand, incorporates the ability to use different sets of hazard-consistent ground motions at different intensity levels, making it an attractive option for collapse risk assessment. This was the reason for its adoption by FEMA P-58 (FEMA 2012) as the recommended procedure to conduct time-based structural performance assessments. Nevertheless, IDA still remains a popular choice due to its simplicity and the relative ease of ground motion selection. The FEMA P695 far field record set is, in fact, often used even when the analysis is not being conducted as part of the FEMA P695 methodology. This paper develops a structural reliability framework that can be used to post-process the results of an IDA and compute a hazard-consistent collapse fragility curve, thus eliminating IDA's biggest shortcoming, and making it a competitive alternative to MSA.

Ground motion selection guidelines provided by current structural design and performance assessment standards are restricted to ensuring the response spectra of the selected ground motions explicitly match site-specific target response spectra (ASCE 2016, FEMA 2012). The response spectrum of a ground motion, which quantifies its amplitude and frequency content, has been shown by a number of studies to be well correlated to the peak deformations and collapse capacity of a structure (Baker and Cornell 2006, Shome et al. 1998), thus justifying its widespread use as a primary ground motion intensity measure. Recent studies have also demonstrated the influence of ground motion duration on structural collapse risk, warranting its consideration in ground motion selection, in addition to response spectra (Chandramohan et al. 2015, Raghunandan and Liel 2013). This paper corroborates the findings of these studies by demonstrating that a ground motion's response spectral shape and duration are both efficient predictors of the lowest intensity it needs to be scaled to, to cause structural collapse, which is known as its collapse intensity. Response spectral shape is quantified using a scalar parameter called  $S_aRatio$  (Eads 2013), and duration using 5-75% significant duration ( $Ds_{5-75}$ ) (Trifunac and Brady 1975). The proposed framework is used to estimate the collapse risk of a ductile eight-story reinforced concrete moment frame building, designed for a site in Seattle, and the results are compared to those obtained by conducting MSA using hazard-consistent ground motions. Ground motion selection procedures that improve the accuracy of collapse risk estimates obtained using the reliability framework, are proposed. Finally, IDA and MSA are unified under the proposed reliability framework, and MSA is shown to represent a simulation-based approach to solve the same problem.

## COMPUTING $S_aRatio$ AND $Ds_{5-75}$ OF A GROUND MOTION

The parameter  $S_aRatio$  was proposed by Eads (2013) as a dimensionless measure of a ground motion's response spectral shape. It is computed as the ratio of the spectral acceleration at a specific period,  $S_a(T)$ , and the geometric mean of the portion of the response spectrum that lies between the periods  $T_{start}$  (usually  $< T$ ) and  $T_{end}$  (usually  $> T$ ), denoted by  $S_{a,avg}(T_{start}, T_{end})$  (Equation 1). Note that 5% damped pseudo-acceleration response spectra are used throughout this paper. Although previous studies have recommended computing  $S_{a,avg}(T_{start}, T_{end})$  as the sample geometric mean of spectral ordinates (Baker and Cornell 2006, Eads et al. 2015), it can, more generally, be computed as the geometric mean of the function  $S_a(T)$  (Equation 2). The trapezoidal rule was used in this study to evaluate the integral numerically.

$$S_aRatio(T, T_{start}, T_{end}) = \frac{S_a(T)}{S_{a,avg}(T_{start}, T_{end})} \quad (1)$$

$$S_{a,avg}(T_{start}, T_{end}) = \exp\left(\frac{\int_{T_{start}}^{T_{end}} \ln S_a(t) dt}{T_{end} - T_{start}}\right) \quad (2)$$

The  $S_aRatio(1.0s, 0.2s, 3.0s)$  value of the ground motion whose response spectrum is shown in Figure 1a is large since it has a large  $S_a(1.0s)$  value and relatively lower spectral ordinates at all

other periods between 0.2s and 3.0s. The opposite is true for the ground motion whose response spectrum is shown in Figure 1b. Eads et al. (2015) recommended using the period range  $0.2T$  to  $3.0T$  to compute  $S_aRatio$  at period  $T$  since it was found to be most efficient in collapse prediction. The parameter  $S_aRatio$  is closely related to  $\varepsilon$  (Baker and Cornell 2005), but offers the advantage of being computable directly from a ground motion time series, without any knowledge of its causal parameters, like magnitude, source-to-site distance, and site  $V_{s30}$  (the average shear wave velocity of the top 30m of the soil profile). Eads (2013) also demonstrated that  $S_aRatio$  is a better predictor of a ground motion's collapse intensity, than  $\varepsilon$ .

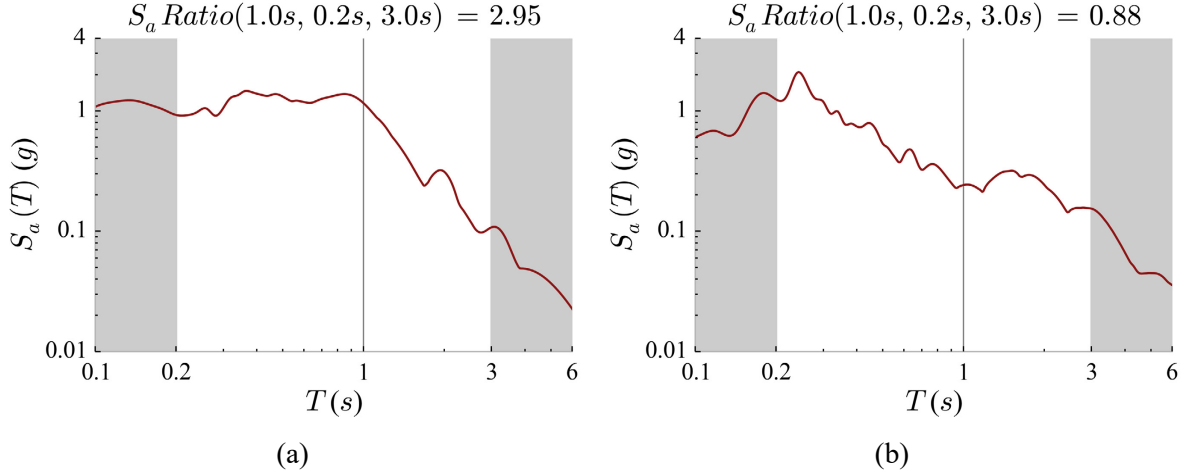


FIGURE 1. Response spectra of two ground motions that have (a) high and (b) low  $S_aRatio(1.0s, 0.2s, 3.0s)$  values respectively. The ground motion in (a) was recorded from the 1999 Duzce, Turkey earthquake, at the Bolu station, and the one in (b) was recorded from the 1979 Imperial Valley earthquake, at the El Centro station. Both are from the FEMA P695 far field set.

The significant duration of a ground motion is defined as the time interval over which a specific percentage of the integral  $\int_0^{t_{max}} a^2(t)dt$  is accumulated, where  $a(t)$  represents the ground acceleration at time  $t$ , and  $t_{max}$  represents the length of the accelerogram. The computation of 5-75% significant duration ( $DS_{5-75}$ ) of an accelerogram is illustrated in Figure 2. Significant duration was preferred over other duration metrics since it was identified to be best suited for ground motion selection for collapse risk assessment by Chandramohan et al. (2015).

### COMPUTING HAZARD-CONSISTENT TARGET DISTRIBUTIONS OF $S_aRatio$ AND $DS_{5-75}$

The procedure to compute hazard-consistent, target probability distributions of  $S_aRatio$  and  $DS_{5-75}$  is an extension of previously developed methods to compute conditional spectra (Jayaram et al. 2011) and the generalized conditional intensity measure (GCIM) (Bradley 2010). These distributions are computed conditional on the exceedance of a primary, amplitude-based ground motion intensity measure, which is quantified by probabilistic seismic hazard analysis (PSHA) (McGuire 2004). The spectral acceleration at the fundamental modal period of the structure under consideration,  $S_a(T_1)$ , is used as the conditioning intensity measure in this study, in line with current structural design practice.

Let the portion of the response spectrum that lies within the range of periods used to compute  $S_aRatio$ ,  $T_{start}$  to  $T_{end}$ , be sampled at  $n$  arbitrarily spaced periods  $t_1, t_2, \dots, t_n$ , where  $t_1 = T_{start}$  and  $t_n = T_{end}$ . Let  $\mathbf{ln IM}$  represent the vector containing the natural logarithms of  $S_a(t_i)$  and  $DS_{5-75}$ .

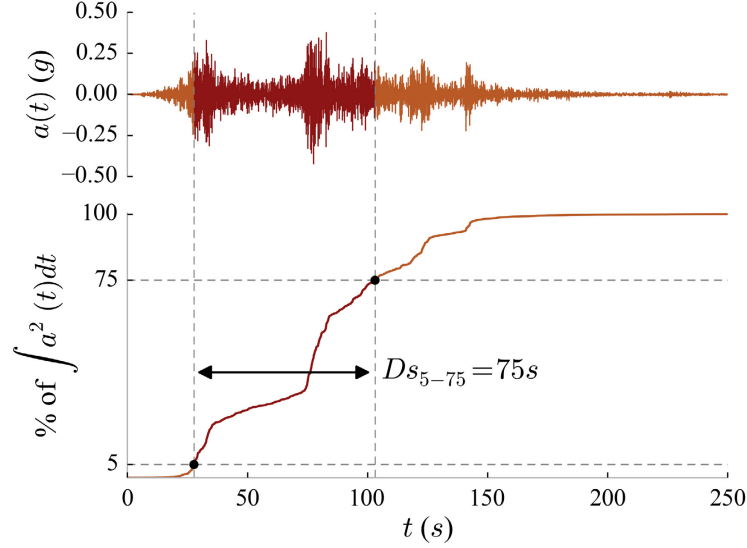


FIGURE 2. (Top) An accelerogram recorded from the 2011 Tohoku earthquake at the Sakunami station, and (Bottom) the normalized, cumulative integral of  $a^2(t)$  illustrating the computation of 5-75% significant duration ( $DS_{5-75}$ ) of the accelerogram

$$\mathbf{\ln IM} = \begin{bmatrix} \ln S_a(t_1) \\ \ln S_a(t_2) \\ \vdots \\ \ln S_a(t_n) \\ \ln DS_{5-75} \end{bmatrix} \quad (3)$$

Since  $S_a(t_i)$  and  $DS_{5-75}$  are usually modeled as lognormal random variables (Abrahamson and Silva 1996),  $\mathbf{\ln IM}$  has a multivariate normal distribution. Computing the mean and covariance of  $\mathbf{\ln IM}$ , conditional on the exceedance of a certain  $S_a(T_1)$  value ( $\mu_{\mathbf{\ln IM}|\ln S_a(T_1)}$  and  $\Sigma_{\mathbf{\ln IM}|\ln S_a(T_1)}$  respectively), requires knowledge of the seismic hazard deaggregation, i.e. the earthquake scenarios that are most likely to cause the exceedance of that  $S_a(T_1)$  value at the site. The conditional mean and covariance of  $\mathbf{\ln IM}$  for each deaggregated earthquake scenario ( $\mu_{\mathbf{\ln IM}(i)|\ln S_a(T_1)}$  and  $\Sigma_{\mathbf{\ln IM}(i)|\ln S_a(T_1)}$  respectively) with relative contribution  $p_i$  can be computed using the computations described in Equations 5 to 9 of Jayaram et al. (2011), with the only difference being that  $\ln DS_{5-75}$  is appended to the vector of logarithms of response spectral ordinates. For a site like Seattle, that receives seismic hazard contributions from different types of seismic sources (interface and in-slab earthquakes from the Cascadia subduction zone and crustal earthquakes from the Seattle fault zone), appropriate models specific to each type of source should be used in the computations. This study uses Campbell and Bozorgnia (2014) to predict response spectral ordinates for crustal earthquakes and Abrahamson et al. (2015) for interface and in-slab earthquakes. Abrahamson and Silva (1996) is used to predict significant duration from all types of seismic sources. The Baker and Jayaram (2008) model for the correlation coefficients between the residuals, or  $\varepsilon$ -values, of response spectral ordinates is used for crustal and in-slab earthquakes, while the Al Atik (2011) model is used for interface earthquakes. The Bradley (2011) model for the correlation coefficients between the residuals of significant duration and response spectral ordinates is used for all types of seismic sources. Note that the Abrahamson and Silva (1996) and Bradley (2011) models for significant duration are used for all types of seismic sources although they were developed only for crustal sources, since similar models for interface and in-slab earthquakes do not currently exist. Although these models are believed to be reasonable for the calculations performed here, additional studies are necessary to verify the validity of their use in this context.

Finally, a weighted average conditional mean and covariance, over all  $m$  deaggregated earthquake scenarios, can be computed using Equations 4 to 6.

$$\boldsymbol{\mu}_{\ln IM | \ln S_a(T_1)} = \sum_{i=1}^m p_i \boldsymbol{\mu}_{\ln IM(i) | \ln S_a(T_1)} \quad (4)$$

$$\boldsymbol{\Sigma}_{\ln IM | \ln S_a(T_1)} = \sum_{i=1}^m p_i [\boldsymbol{\Sigma}_{\ln IM(i) | \ln S_a(T_1)} + \Delta \boldsymbol{\mu}_{\ln IM(i) | \ln S_a(T_1)} \Delta \boldsymbol{\mu}_{\ln IM(i) | \ln S_a(T_1)}^T] \quad (5)$$

$$\Delta \boldsymbol{\mu}_{\ln IM(i) | \ln S_a(T_1)} = \boldsymbol{\mu}_{\ln IM(i) | \ln S_a(T_1)} - \boldsymbol{\mu}_{\ln IM | \ln S_a(T_1)} \quad (6)$$

The conditional distribution of  $\ln S_a \text{Ratio}$  is also normal since it can be shown to be an affine function of other normal random variables. Taking the natural logarithm of Equations 1 and 2, we get

$$\ln S_a \text{Ratio}(T, T_{start}, T_{end}) = \ln S_a(T_1) - \frac{\int_{T_{start}}^{T_{end}} \ln S_a(t) dt}{T_{end} - T_{start}} \quad (7)$$

Using any linear numerical integration rule to evaluate the integral in Equation 7,

$$\int_{T_{start}}^{T_{end}} \ln S_a(t) dt = \sum_{i=1}^n \alpha_i \ln S_a(t_i) \quad (8)$$

where the  $\alpha_i$  depend on the specific numerical integration rule employed. For the trapezoidal rule used in this study,  $\alpha_1 = t_2 - t_1/2$ ,  $\alpha_2 = t_3 - t_1/2$ ,  $\alpha_3 = t_4 - t_2/2$ , ...,  $\alpha_{n-1} = t_n - t_{n-2}/2$ , and  $\alpha_n = t_n - t_{n-1}/2$ . It is important to note that  $\ln S_a(T_1)$  in Equation 7 is not random since it is the conditioning intensity measure. Let  $\ln im$  represent the vector containing the natural logarithms of  $S_a \text{Ratio}$  and  $DS_{5-75}$ .

$$\ln im = \begin{bmatrix} \ln S_a \text{Ratio} \\ \ln DS_{5-75} \end{bmatrix} \quad (9)$$

Using Equations 3, 7, 8, and 9,  $\ln im | \ln S_a(T_1)$  can be written as an affine transformation of  $\ln IM | \ln S_a(T_1)$  using the following matrix equations

$$\ln im | \ln S_a(T_1) = \mathbf{A} \ln IM | \ln S_a(T_1) + \mathbf{b} \quad (10)$$

$$\mathbf{A} = \begin{bmatrix} -\frac{\alpha_1}{T_{end} - T_{start}} & -\frac{\alpha_2}{T_{end} - T_{start}} & \dots & -\frac{\alpha_n}{T_{end} - T_{start}} & 0 \\ 0 & 0 & \dots & 0 & 1 \end{bmatrix} \quad (11)$$

$$\mathbf{b} = \begin{bmatrix} \ln S_a(T_1) \\ 0 \end{bmatrix} \quad (12)$$

The conditional mean and covariance of  $\ln im$  are now given by

$$\boldsymbol{\mu}_{\ln im | \ln S_a(T_1)} = \mathbf{A} \boldsymbol{\mu}_{\ln IM | \ln S_a(T_1)} + \mathbf{b} \quad (13)$$

$$\boldsymbol{\Sigma}_{\ln im | \ln S_a(T_1)} = \mathbf{A} \boldsymbol{\Sigma}_{\ln IM | \ln S_a(T_1)} \mathbf{A}^T \quad (14)$$

with  $\boldsymbol{\mu}_{\ln IM | \ln S_a(T_1)}$  and  $\boldsymbol{\Sigma}_{\ln IM | \ln S_a(T_1)}$  given by Equations 4 and 5 respectively. These equations, thus, fully define the hazard-consistent joint target distribution of  $S_a \text{Ratio}$  and  $DS_{5-75}$ , conditional on the exceedance of any ground motion intensity level. Note that computing the conditional mean target  $S_a \text{Ratio}$  using Equation 13 is equivalent to computing the  $S_a \text{Ratio}$  value directly from the conditional mean spectrum (CMS) (Baker 2011).

The median  $S_aRatio(1.76s, 0.35s, 5.00s)$  and  $DS_{5-75}$  targets, conditional on the exceedance of a range of  $S_a(1.76s)$  values in Seattle are plotted in Figure 3. The period 1.76s corresponds to the fundamental modal period of the reinforced concrete moment frame building used in this study.  $S_aRatio$  was computed only until 5.00s instead of  $3.0T_1 = 5.28s$  since the Al Atik (2011) model does not provide correlation coefficients for response spectral ordinates at periods above 5.00s. This is, however, not expected to alter the obtained results. Smoothing splines were used to linearly extrapolate these targets to higher ground motion intensity levels, for which deaggregation information was not available. The amount of extrapolation required in the computations described below was small, and was judged to be reasonable. The increasing trends in Figure 3 indicate that ground motions with large intensities tend to have more peaked response spectra (as indicated by the CMS) and longer durations.

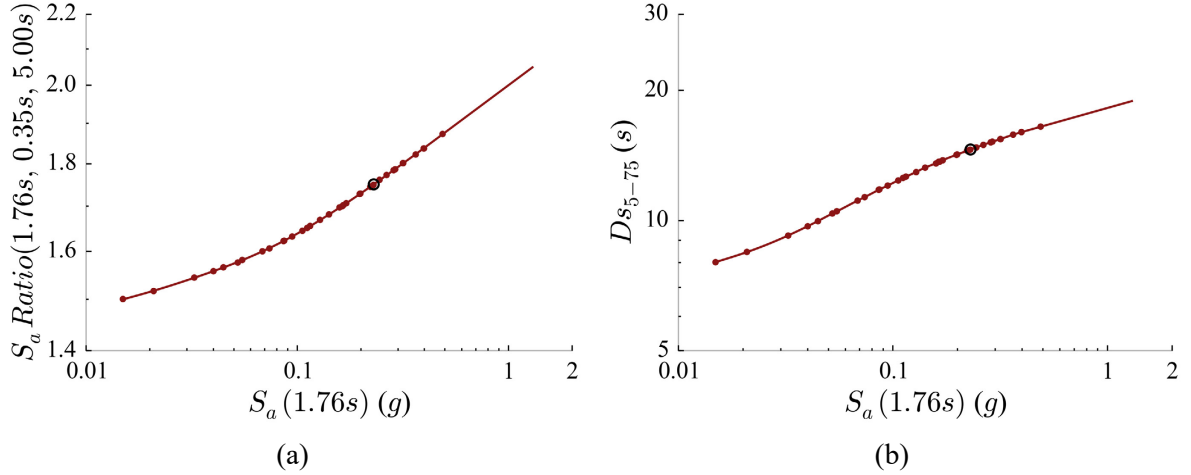


FIGURE 3. Median (a)  $S_aRatio(1.76s, 0.35s, 5.00s)$  and (b)  $DS_{5-75}$  targets, conditional on the exceedance of different  $S_a(1.76s)$  values at Seattle. The points represent intensity levels at which deaggregation information was available, and the curve is a smoothing spline used to linearly extrapolate the targets to higher intensity levels.  $MCE_R$  level targets are shown as black circles.

## COLLAPSE RISK ASSESSMENT USING THE STRUCTURAL RELIABILITY FRAMEWORK

A ductile eight-story reinforced concrete moment frame building, designed for a site in Seattle, was used to demonstrate the application of the proposed structural reliability framework for collapse risk estimation. A two-dimensional numerical model of the structure was created and analyzed in OpenSees rev. 5184 (McKenna et al. 2006). The model was developed by Raghunandan et al. (2014) to study the collapse risk of structures in the Pacific Northwest. The beams and columns of the frame were modeled using linear elastic elements, with zero-length plastic hinges located at each end. The hysteretic behavior of the hinges was modeled using the Modified Ibarra-Medina-Krawinkler peak-oriented model (Ibarra et al. 2005), which includes a post-peak negative stiffness branch of the backbone curve to capture in-cycle deterioration, as well as cyclically deteriorating strength and stiffness based on the cumulative hysteretic energy dissipated. Finite panel zones were modeled, with their shear deformations represented by a trilinear backbone curve. The contribution of the adjacent gravity system to the destabilizing  $P - \Delta$  effect was modeled using a pin-connected leaning column. Previous studies have demonstrated that the deterioration in strength and stiffness of structural components at large inelastic deformations, as well as the destabilizing effect of gravity loads, need to be modeled to capture the effect of ground motion duration on structural response (Chandramohan et al. 2015, Raghunandan and Liel 2013). The structure is assumed to be located on a site with  $V_{S30} = 760m/s$ .

A set of 88 ground motions was chosen to analyze the structure. 44 of these ground motions were taken from the FEMA P695 far field set. Since all of these ground motions are of comparatively short duration, the record set was supplemented with 44 long duration ground motions with  $DS_{5-75} > 25s$  recorded from large magnitude interface earthquakes like the 2011 Tohoku (Japan), 2010 Maule (Chile), 2003 Hokkaido (Japan), 1985 Michoacan (Mexico), and 1985 Valparaiso (Chile) earthquakes. The proposed framework, though, is general, and can be used with any set of ground motions subject to a few selection guidelines described below. The set of 88 ground motions was used to conduct IDA on the structural model. Each ground motion was scaled to incrementally higher intensity levels until structural collapse, indicated by the exceedance of a peak story drift ratio (SDR) of 0.10, was observed. The collapse intensity of each ground motion, computed as its  $S_a(T_1)$  value when scaled to the lowest intensity level required to cause structural collapse, was noted.

### Computing the failure surface

The failure surface is estimated by fitting the following multiple linear regression equation to the IDA results using the least-squares method

$$\ln S_a(T_1) \text{ at collapse} = \gamma_0 + \gamma_1 \ln S_aRatio + \gamma_2 \ln DS_{5-75} + \epsilon \quad (15)$$

where  $\epsilon$  represents the error. This error term is assumed to be normally distributed with zero mean and standard deviation  $\sigma$ , which can be estimated as

$$\hat{\sigma} = \sqrt{\frac{RSS}{n_{gm} - 3}} \quad (16)$$

where  $RSS$  represents the sum of the squares of the residuals and  $n_{gm}$  is the number of ground motions used in the analysis. The estimated failure surface is plotted in Figure 4. The coefficient of determination ( $R^2$ ) from the regression analysis was computed to be 0.81, which implies that  $S_aRatio$  and  $DS_{5-75}$ , together explain 81% of the variance in the ground motion collapse intensities. The  $R^2$  was computed to be 0.45 when using only  $S_aRatio$  in the regression equation, and 0.40 when using only  $DS_{5-75}$ , indicating that they each contribute almost equal predictive power to the regression

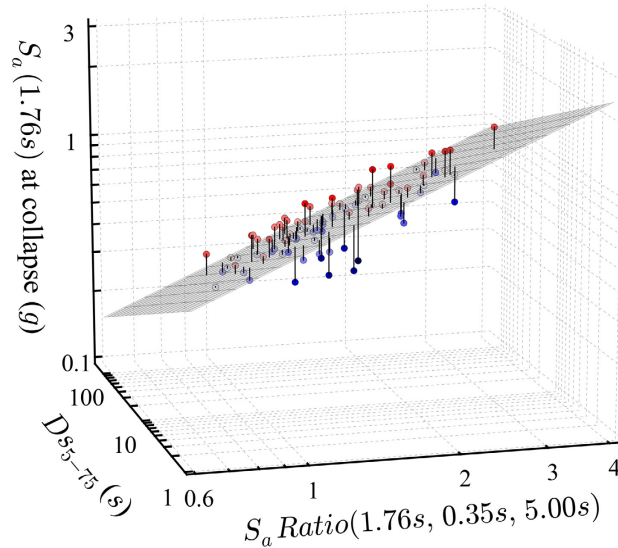


FIGURE 4. Failure surface for the reinforced concrete moment frame building, estimated by fitting a multiple linear regression equation to the IDA results. The vertical lines represent the residuals.

equation involving them both. The failure surface can now be used to compute the probability that a ground motion with a certain  $S_aRatio$  and  $DS_{5-75}$ , when scaled to a certain  $S_a(T_1)$  value, will cause structural collapse

$$P[collapse | \ln S_aRatio, \ln DS_{5-75}, \ln S_a(T_1)] = \Phi \left[ \frac{\ln S_a(T_1) - (\gamma_0 + \gamma_1 \ln S_aRatio + \gamma_2 \ln DS_{5-75})}{\hat{\sigma}} \right] \quad (17)$$

where  $\hat{\sigma}$  is computed using Equation 16 and  $\Phi$  represents the standard normal cumulative distribution function. The probability of causing collapse is equal to 0.5 when the ground motion is scaled so that its  $S_a(T_1)$  value lies exactly on the failure surface. This probability approaches 0 at lower intensity levels, and 1 at higher intensity levels.

### Computing the hazard-consistent collapse fragility curve

A collapse fragility curve quantifies the probability of collapse as a function of the ground motion intensity level. The probability of collapse at any  $S_a(T_1)$  level can be computed by numerically evaluating the following reliability integral

$$P[collapse | \ln S_a(T_1)] = \iint P[collapse | \ln S_aRatio, \ln DS_{5-75}, \ln S_a(T_1)] f[\ln S_aRatio, \ln DS_{5-75} | \ln S_a(T_1)] d \ln S_aRatio d \ln DS_{5-75} \quad (18)$$

where  $P[collapse | \ln S_aRatio, \ln DS_{5-75}, \ln S_a(T_1)]$  is computed using Equation 17 and  $f[\ln S_aRatio, \ln DS_{5-75} | \ln S_a(T_1)]$  represents the probability density function of a bivariate normal distribution whose mean,  $\mu_{\ln im | \ln S_a(T_1)}$ , and covariance,  $\Sigma_{\ln im | \ln S_a(T_1)}$ , are given by Equations 13 and 14 respectively. The two terms in the integrand of the reliability integral, conditional on two different ground motion intensity levels, are illustrated in Figure 5.  $f[\ln S_aRatio, \ln DS_{5-75} | \ln S_a(T_1)]$  represents the distribution of the characteristics of the anticipated ground motions, and is depicted by the elliptical contours.  $P[collapse | \ln S_aRatio, \ln DS_{5-75}, \ln S_a(T_1)]$  represents the probability of observing structural collapse as a function of the ground motion characteristics, and is depicted by the linear contours. The overlap of the contours indicates that collapses are more likely to occur at the higher intensity level, as expected. Note that Equation 18 is similar to Equations 20 and 21 from Baker (2007), but this study improves upon it in a number of ways, most importantly by identifying  $S_aRatio$  and  $DS_{5-75}$  as efficient predictors of a ground motion's collapse intensity.

A non-parametric collapse fragility curve, computed by evaluating this integral at multiple intensity levels, is plotted in Figure 6, and the mean annual frequency of collapse computed by integrating it with the seismic hazard curve is indicated in the legend. It is found to compare well to the fragility curve obtained by conducting MSA using 100 hazard-consistent ground motions per intensity level, selected to match source-specific target distributions of response spectra and duration as per the procedure outlined in Chandramohan et al. (2014). In fact, MSA can be seen to represent a simulation-based approach to evaluate the reliability integral in Equation 18. Selecting hazard-consistent ground motions at an intensity level is equivalent to simulating  $S_aRatio$  and  $DS_{5-75}$  values from the distribution  $f[\ln S_aRatio, \ln DS_{5-75} | \ln S_a(T_1)]$ . Computing the probability of collapse as the fraction of these ground motions that cause structural collapse is equivalent to integrating it with  $P[collapse | \ln S_aRatio, \ln DS_{5-75}, \ln S_a(T_1)]$  over all  $S_aRatio$  and  $DS_{5-75}$  values. Viewing MSA in this context provides a number of opportunities to improve its efficiency by selecting ground motions using importance sampling techniques, wherein ground motions with lower  $S_aRatio$  values and longer durations are intentionally selected at each intensity level so as to simulate more collapses. The fragility curve computed using the popular maximum likelihood estimation method, which entails fitting the moments of a lognormal distribution to the sample moments of the ground motion collapse intensities,



is found to over-estimate the collapse risk significantly. The fragility curve obtained by adjusting the median collapse capacity estimated using only the FEMA P695 far field set, by a spectral shape factor as per FEMA P695, on the other hand, is found to significantly under-estimate the collapse risk.

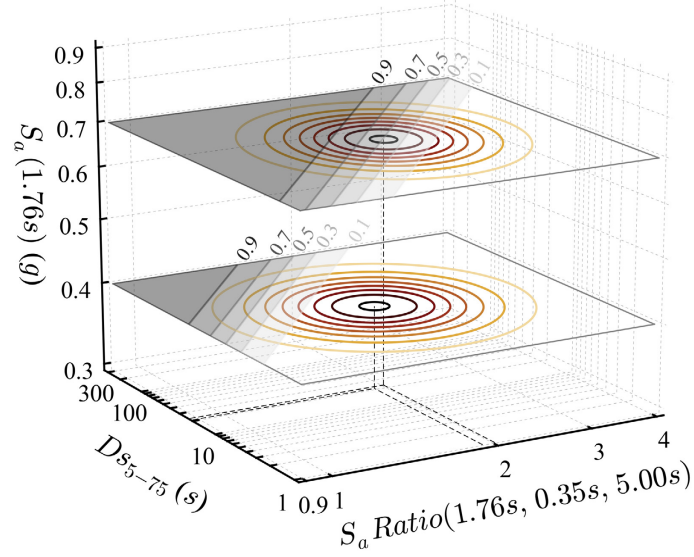


FIGURE 5. A schematic illustrating the terms in the integrand of the reliability integral (Equation 18), conditional on two ground motion intensity levels in Seattle:  $S_a(1.76s) = 0.4g$  and  $0.7g$

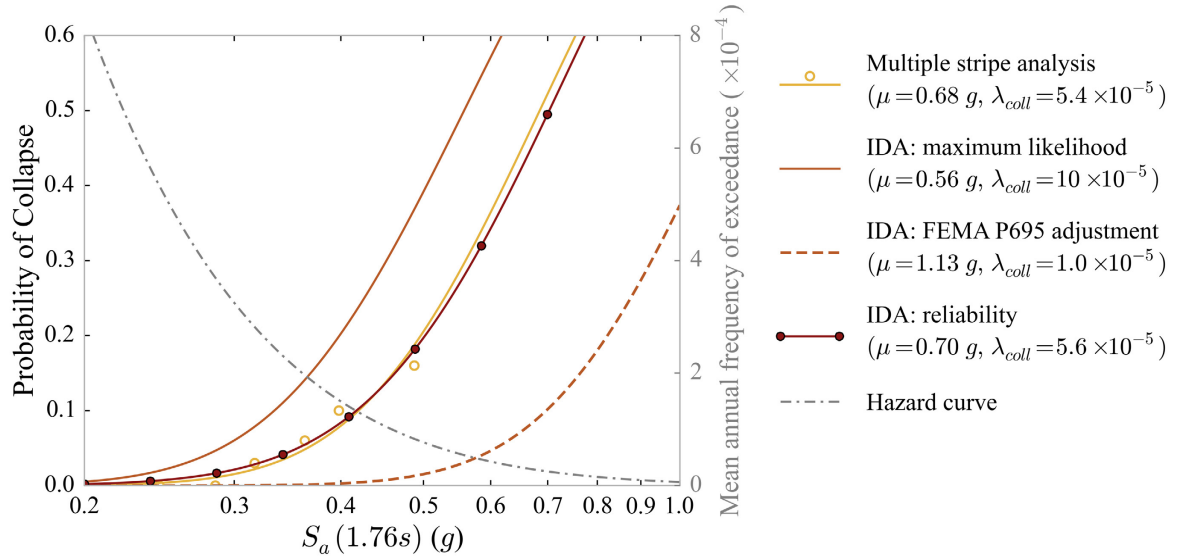


FIGURE 6. Comparison of the collapse fragility curves (medians denoted as  $\mu$ ) and mean annual frequencies of collapse ( $\lambda_{coll}$ ) estimated using different methods

### Recommendations for ground motion selection

The objective of any ground motion selection strategy used in conjunction with the reliability framework should be to minimize the uncertainty in predicting the height of the failure surface ( $\ln S_a(T_1)$  at collapse) in the range of  $S_a Ratio$  and  $Ds_{5-75}$  values of the ground motions anticipated at the site. Thus, the selection of ground motions can be viewed as an experimental design problem (Kutner et al. 2004). The contours in Figure 7 represent the standard error in predicting the height of

the failure surface. The standard error is observed to be the least at the sample geometric mean  $S_aRatio$  and  $DS_{5-75}$  of all the ground motions, and to increase radially outwards. The selected ground motions should, therefore, have geometric mean  $S_aRatio$  and  $DS_{5-75}$  values near the corresponding median targets conditional on all ground motion intensity levels that contribute significantly to the collapse risk of the structure. The median targets conditional on the risk-targeted maximum considered earthquake ( $MCE_R$ ) level (ASCE 2016), and the median collapse capacity level estimated using the reliability method, are superimposed on the contours and found to lie reasonably close to the geometric mean values. It is also important to ensure that the marginal distributions of  $S_aRatio$  and  $DS_{5-75}$  of the selected ground motions have a large variance relative to the variance of the corresponding targets. Orthogonality can be introduced into the ground motion selection procedure by selecting pairs of records with the same  $S_aRatio$  value but different  $DS_{5-75}$  values or vice versa, thus further lowering prediction standard errors. Finally using more ground motions will produce more precise predictions.

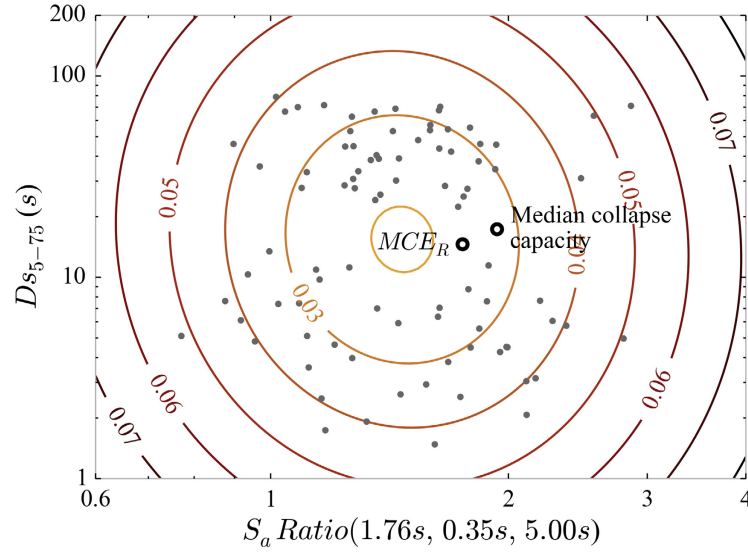


FIGURE 7. Contours of the standard error in predicting the height of the failure surface ( $\ln S_a(1.76s)$  at collapse), with the  $S_aRatio$  and  $DS_{5-75}$  values of the selected ground motions, and the median targets conditional on the  $MCE_R$  intensity level ( $S_a(1.76s) = 0.23g$ ) and median collapse capacity intensity level ( $S_a(1.76s) = 0.70g$ ) superimposed

## CONCLUSION

A structural reliability framework was developed to post-process the results of an incremental dynamic analysis (IDA) and compute a hazard-consistent collapse fragility curve. This resolves a major drawback of the IDA procedure, making it a competitive alternative to multiple stripe analysis (MSA). The proposed procedure employs a scalar parameter called  $S_aRatio$  that quantifies response spectral shape, and 5-75% significant duration ( $DS_{5-75}$ ) as secondary intensity measures. These two parameters are shown to be good predictors of a ground motion's collapse intensity. They are demonstrated to be capable of explaining 81% of the variance in the collapse intensities of the ground motions used to analyze a ductile eight-story reinforced concrete moment frame building, designed for a site in Seattle. This highlights the importance of considering ground motion duration and response spectral shape in structural collapse risk assessment.  $S_aRatio$  and  $DS_{5-75}$  are used in conjunction with  $S_a(T_1)$  to define a linear failure surface using the results of an IDA. Hazard-consistent target distributions of  $S_aRatio$  and  $DS_{5-75}$ , conditional on the exceedance of an intensity level, are integrated with the failure surface to estimate the probability of observing structural collapse at that intensity level. Evaluating this

reliability integral at many different intensity levels allows computing a hazard-consistent collapse fragility curve, which, for the case of the reinforced concrete moment frame analyzed in this study, was found to agree well with the fragility curve computed by conducting MSA using hazard-consistent ground motions. The fragility curve computed using the popular maximum likelihood method was found to significantly over-estimate the collapse risk. Adjusting the median collapse capacity using a spectral shape factor, as recommended by FEMA P695 was, on the other hand, found to significantly under-estimate the collapse risk. Finally, IDA and MSA were united under the structural reliability framework, and were shown to represent two different approaches to solving the same problem.

## ACKNOWLEDGEMENTS

This work was supported by the State of California through the Transportation Systems Research Program of the Pacific Earthquake Engineering Research Center (PEER) and by Stanford University. Any opinions, findings, conclusions, and recommendations expressed in this material are those of the author, and do not necessarily reflect those of the funding agencies. I would like to thank my doctoral advisors—Prof. Greg Deierlein and Prof. Jack Baker—for their support and guidance. I also thank Meera Raghunandan and Abbie Liel for sharing the model of the moment frame building.

## REFERENCES

- Abrahamson, N. A., and Silva, W. J. (1996). *Empirical Ground Motion Models*. Report to Brookhaven National Laboratory, Upton, NY.
- Abrahamson, N., Gregor, N., and Addo, K. (2015). “BC Hydro Ground Motion Prediction Equations For Subduction Earthquakes (in press).” *Earthquake Spectra*, Earthquake Engineering Research Institute.
- ASCE. (2016). *Minimum Design Loads for Buildings and Other Structures (in press)*. American Society of Civil Engineers, Reston, VA.
- Al Atik, L. (2011). “Correlation of Spectral Acceleration Values for Subduction and Crustal Models.” *COSMOS Technical Session*, Emeryville, CA.
- Baker, J. W. (2007). “Probabilistic structural response assessment using vector-valued intensity measures.” *Earthquake Engineering & Structural Dynamics*, John Wiley & Sons, Inc., 36(13), 1861–1883.
- Baker, J. W. (2011). “Conditional Mean Spectrum: Tool for Ground-Motion Selection.” *Journal of Structural Engineering*, 137(3), 322–331.
- Baker, J. W., and Cornell, C. A. (2005). “A vector-valued ground motion intensity measure consisting of spectral acceleration and epsilon.” *Earthquake Engineering & Structural Dynamics*, 34(10), 1193–1217.
- Baker, J. W., and Cornell, C. A. (2006). “Spectral shape, epsilon and record selection.” *Earthquake Engineering & Structural Dynamics*, 35(9), 1077–1095.
- Baker, J. W., and Jayaram, N. (2008). “Correlation of Spectral Acceleration Values from NGA Ground Motion Models.” *Earthquake Spectra*, 24(1), 299–317.
- Bommer, J. J., and Acevedo, A. B. (2004). “The Use of Real Earthquake Accelerograms as Input to Dynamic Analysis.” *Journal of Earthquake Engineering*, 8(1), 43–91.
- Bradley, B. A. (2010). “A generalized conditional intensity measure approach and holistic ground-motion selection.” *Earthquake Engineering & Structural Dynamics*, 39(12), 1321–1342.
- Bradley, B. A. (2011). “Correlation of Significant Duration with Amplitude and Cumulative Intensity Measures and Its Use in Ground Motion Selection.” *Journal of Earthquake Engineering*, 15(6), 809–832.
- Campbell, K. W., and Bozorgnia, Y. (2014). “NGA-West2 Ground Motion Model for the Average

Horizontal Components of PGA, PGV, and 5% Damped Linear Acceleration Response Spectra.” *Earthquake Spectra*, Earthquake Engineering Research Institute, 30(3), 1087–1115.

Chandramohan, R., Baker, J. W., and Deierlein, G. G. (2014). “Hazard-consistent Ground Motion Duration: Calculation Procedure and Impact on Structural Collapse Risk.” *10th U.S. National Conference on Earthquake Engineering*, Anchorage, AK.

Chandramohan, R., Baker, J. W., and Deierlein, G. G. (2015). “Quantifying the influence of ground motion duration on structural collapse capacity using spectrally equivalent records (in press).” *Earthquake Spectra*, Earthquake Engineering Research Institute.

Eads, L. (2013). “Seismic Collapse Risk Assessment of Buildings: Effects of Intensity Measure Selection and Computational Approach.” Stanford University.

Eads, L., Miranda, E., and Lignos, D. G. (2015). “Average spectral acceleration as an intensity measure for collapse risk assessment.” *Earthquake Engineering & Structural Dynamics*, 44(12), 2057–2073.

FEMA. (2009). *Quantification of Building Seismic Performance Factors*. Federal Emergency Management Agency, Washington, D.C.

FEMA. (2012). *Seismic Performance Assessment of Buildings, Volume 1 - Methodology*. Federal Emergency Management Agency, Washington, D.C.

Ibarra, L. F., Medina, R. A., and Krawinkler, H. (2005). “Hysteretic models that incorporate strength and stiffness deterioration.” *Earthquake Engineering & Structural Dynamics*, 34(12), 1489–1511.

Jalayer, F. (2003). “Direct probabilistic seismic analysis: Implementing non-linear dynamic assessments.” Ph.D. Dissertation, Stanford University.

Jayaram, N., Lin, T., and Baker, J. W. (2011). “A Computationally efficient ground-motion selection algorithm for matching a target response spectrum mean and variance.” *Earthquake Spectra*, 27(3), 797–815.

Katsanos, E. I., Sextos, A. G., and Manolis, G. D. (2010). “Selection of earthquake ground motion records: A state-of-the-art review from a structural engineering perspective.” *Soil Dynamics and Earthquake Engineering*, 30(4), 157–169.

Kutner, M. H., Nachtsheim, C., and Neter, J. (2004). *Applied Linear Regression Models*. McGraw-Hill/Irwin.

Lin, T., Haselton, C. B., and Baker, J. W. (2013). “Conditional spectrum-based ground motion selection. Part I: Hazard consistency for risk-based assessments.” *Earthquake Engineering & Structural Dynamics*, 42(12), 1847–1865.

McGuire, R. K. (2004). *Seismic hazard and risk analysis*. Earthquake Engineering Research Institute, Oakland, CA.

McKenna, F., Fenves, G. L., and Scott, M. H. (2006). “OpenSees: Open system for earthquake engineering simulation.” University of California, Berkeley, CA.

Raghunandan, M., and Liel, A. B. (2013). “Effect of ground motion duration on earthquake-induced structural collapse.” *Structural Safety*, 41, 119–133.

Raghunandan, M., Liel, A. B., and Luco, N. (2014). “Collapse Risk of Buildings in the Pacific Northwest Region due to Subduction Earthquakes (in press).” *Earthquake Spectra*, Earthquake Engineering Research Institute.

Shome, N., Cornell, C. A., Bazzurro, P., and Carballo, J. E. (1998). “Earthquakes, Records, and Nonlinear Responses.” *Earthquake Spectra*, 14(3), 469–500.

Trifunac, M. D., and Brady, A. G. (1975). “A study on the duration of strong earthquake ground motion.” *Bulletin of the Seismological Society of America*, 65(3), 581–626.

Vamvatsikos, D., and Cornell, C. A. (2002). “Incremental dynamic analysis.” *Earthquake Engineering & Structural Dynamics*, 31(3), 491–514.